Finite-temperature properties of perfect crystals and defects from zero-temperature energy minimization

J M Rickman†, R Najafabadi†, L Zhao‡ and D J Srolovitz†‡

† Department of Materials Science and Engineering, University of Michigan, Ann Arbor, MI 48109-2136, USA
‡ Applied Physics Program, University of Michigan, Ann Arbor, MI 48109-2136, USA

Abstract. A method for calculating the thermodynamic properties of both classical perfect crystals and defects by performing a *single* zero-temperature energy minimization is described. This method is based upon the calculation of a local harmonic free energy as performed by LeSar *et al* and by Sutton, and involves determining the dynamical matrix, Gruneisen parameters, and the elastic properties of the system. The dependence of the free energy and the lattice parameter of a perfect Au crystal on temperature are accurately determined with this method. The validity of this method is demonstrated by accurately determining the temperature dependence of the vacancy formation energy, the excess free energy of a (100) surface, and the excess free energy of a Σ13 [001] (22.62°) twist grain boundary.

1. Introduction

Atomistic computer simulations are currently employed to determine the structural and thermodynamic properties of solids and their defects over a wide range of temperature and pressure. For example, the free energy (see, e.g. [1]), elastic properties [2], and point-defect formation free energies [3] of crystalline solids have been determined by using Monte Carlo (MC) and molecular dynamics (MD) methods. Such methods, while ideally suited to these calculations, have the disadvantage of requiring appreciable computational resources in order to determine the requisite ensemble, or equivalently, long-time averages.

In order to overcome this disadvantage and thereby permit a reasonably quick, but accurate, determination of the properties of interest, a new method was introduced for calculating the thermodynamic properties of solids, perfect or with defects, by minimizing the local harmonic (LH) free energy of the system with respect to the coordinates of its constituent atoms at the desired temperature [4, 5]. This LH free-energy minimization method is computationally efficient because the vibrational spectrum of the N atoms constituting the solid is described by N 3×3 *local* dynamical matrices, as opposed to the full $3N \times 3N$ dynamical matrix. This simplification of the harmonic approximation, which neglects the explicit vibrational coupling of the atoms, leads to a LH free energy that simply depends on the product of the determinants of the N local dynamical matrices. Hence, the minimization of the free energy with respect to the atomic coordinates requires only the calculation of the determinants of N 3×3 matrices at each step. Thus, the temperature dependence of quantities

such as the free energy, the entropy and the zero-pressure volume of a solid can now be determined from a *series* of LH free-energy minimizations performed at different temperatures.

It is clear that the computational efficiency of the free-energy minimization method could be further enhanced if it were possible to perform, instead, a *single* energy minimization, say at zero temperature, and obtain, for example, the free energy and other thermodynamic properties over a wide range of temperature. Some recent work involving the calculation of the specific heat of spin systems [6] and the free energy of homogeneous solids [7] at finite temperatures by using the MC method suggests that this is, indeed, possible. In these MC investigations the properties of the system of interest were determined over a wide range of temperature from a single simulation performed at some reference temperature by analysing the probability distribution for the energy obtained in the simulation at the reference temperature. In this work we shall implement these ideas within the framework of the LH free-energy minimization method. In particular, the dependence of the volume, and hence of the free energy, of a solid on temperature will be expressed in terms of the zero-temperature vibrational spectrum of the solid and various volume derivatives of the (local) atomic vibrational frequencies. It will also be shown that, with this information, one can even determine the temperature dependence of the properties of both point and extended defects.

This paper is organized as follows. In section 2 we use the isobaric-canonical ensemble to derive an expression for the temperature dependence of the average volume, $\langle V \rangle(T)$, of a solid. This result is then employed to calculate the local harmonic free energy, F_{LH}, for the solid. In section 3 this approach is applied to the determination of the temperature dependence of $\langle V \rangle$ and F_{LH} for solid Au as modelled by an embedded-atom method (EAM) potential. We also demonstrate that the vacancy formation energy, the excess free energy of a (100) free surface, and the excess free energy of a $\Sigma 13$ [001] (22.62°) twist grain boundary in EAM Au can be accurately determined from zero-temperature information. The implications of these results are discussed in section 4.

2. Method

2.1. Calculation of temperature derivatives of the volume

Consider a classical solid of volume V at zero pressure and fixed temperature T which consists of N atoms with fixed centres of mass. This system can be viewed, to a reasonable approximation, as a collection of oscillators each vibrating about its average atomic position. A LH description of this system requires a knowledge of the three (possibly degenerate) eigenfrequencies $\omega_{\alpha i}(\alpha = 1, 2, 3)$ for each atom i. The LH free energy A of this crystal [4] is given by

$$A(T, V) = U + 3k_B T \sum_{i=1}^{N} \ln \left(\frac{h D_i^{1/6}}{2\pi k_B T} \right) \tag{1}$$

where $D_i = (\omega_{1i}\omega_{2i}\omega_{3i})^2$ is the determinant of the local dynamical matrix of the atom i. The free-energy minimization method [4] can be used to determine the equilibrium structure of the solid at various temperatures, and hence its free energy,

by performing a series of minimizations of A with respect to the atomic coordinates at different temperatures. For the case of a perfect crystal the free-energy minimization method yields the temperature dependence of the zero-pressure volume $\langle V \rangle$ of the system.

The temperature dependence of $\langle V \rangle$ can also be obtained, with a reasonable accuracy, from the results of a single zero-temperature energy minimization. In order to see this, first observe that if the volume of the solid V_0 and its temperature derivatives at zero temperature are known, then $\langle V \rangle$ can be determined at higher temperatures from the Maclaurin series expansion

$$\langle V \rangle = V_0 + \sum_{n=1}^{\infty} \left(\frac{1}{n!} \right) \left(\frac{\partial^n \langle V \rangle}{\partial T^n} \right)_0 T^n \tag{2}$$

where the temperature derivatives are to be evaluated at $T = 0$.

The temperature derivatives in equation (2) can be calculated by using the isobaric-canonical ensemble from statistical mechanics [8]. One finds that

$$\langle V \rangle = V_0 + \int_{-\infty}^{\infty} d(\Delta V) \exp[-\beta A(\Delta V)] \Delta V \Big/ \left\{ \int_{-\infty}^{\infty} d(\Delta V) \exp[-\beta A(\Delta V)] \right\} \tag{3}$$

where $\Delta V = V - V_0$, $\beta = 1/k_B T$, the applied pressure is zero, and the volume dependence of A is indicated explicitly. Upon substituting equation (1) into equation (3) one obtains

$$\langle V \rangle = V_0 + \int_{-\infty}^{\infty} d(\Delta V) \exp(-\beta U) f(\omega) \Delta V \Big/ \left\{ \int_{-\infty}^{\infty} d(\Delta V) \exp(-\beta U) f(\omega) \right\} \tag{4}$$

where $f(\omega) = \prod_{i=1}^{N} (D_i)^{-1/2} = \prod_{i=1}^{N} (\omega_{1i} \omega_{2i} \omega_{3i})^{-1}$.

In order to calculate the temperature dependence of $\langle V \rangle$ at low temperatures, it is necessary to expand the functions in the integrand in equation (4) about V_0. Upon expanding both U and $f(\omega)$ in ΔV one obtains

$$U = U(V_0) + \tfrac{1}{2} \left(\partial^2 U / \partial V^2 \right)_0 (\Delta V)^2 + \tfrac{1}{6} \left(\partial^3 U / \partial V^3 \right)_0 (\Delta V)^3 + \ldots \tag{5a}$$

$$f(\omega) = f(\omega)|_0 + (\partial f(\omega) / \partial V)_0 (\Delta V) + \tfrac{1}{2} \left(\partial^2 f(\omega) / \partial V^2 \right)_0 (\Delta V)^2 + \ldots \tag{5b}$$

where the linear term in equation (5a) is absent since the pressure is taken to be zero. If equation (5a) is truncated after the cubic term, then equation (4) can be written as the ratio of Gaussian integrals (by treating the cubic term as a perturbation) and evaluated to the desired order in temperature. One finds that

$$\langle (V - V_0) \rangle \approx [C_1(k_B T) + C_2(k_B T)^2] / [1 + C_3(k_B T)] \tag{6}$$

where

$$C_1 = (f'(\omega)/f(\omega_0))(1/U'') - \tfrac{1}{2} U''' / (U'')^2 \tag{7a}$$

$$C_2 = (f'''(\omega)/f(\omega_0)) \left(\frac{1}{U''} \right)^2 - \tfrac{5}{4} (U''' / (U'')^3) f''(\omega) / f(\omega_0) \tag{7b}$$

$$C_3 = (f''(\omega)/2f(\omega_0)) 1/U'' - \tfrac{1}{2} (f'(\omega)/f(\omega_0)) U''' / (U'')^2 \tag{7c}$$

and the primes denote differentiation with respect to the volume. The resulting model incorporates anharmonicity, and therefore thermal expansion, through $(\partial^3 U/\partial V^3)_0$ and the volume derivatives of $f(\omega)$. It should be noted that, although the terms $(\partial^n U/\partial V^n)_0 \, (n \geqslant 4)$ are present in the perturbation expansion, they only contribute terms of order $1/N$ to the thermal expansion and higher temperature derivatives of $\langle V \rangle$.

The first temperature derivative of the volume (in the limit $N \to \infty$) at zero temperature is found to be

$$\alpha \equiv (1/V)(\partial V/\partial T)_0 = (k_B \Gamma / BV) \tag{8}$$

where α is the thermal expansion parameter, B is the zero-temperature bulk modulus, and $\Gamma \equiv -(V/f(\omega))(\partial f(\omega)/\partial V)_0$. The quantities on the right-hand side of equation (8) are to be evaluated at zero temperature. α is, in general, not zero since our system is classical and anharmonic. For a perfect Einstein crystal with a single frequency ω, $\Gamma = 3N\gamma$ where $\gamma \equiv -(V/\omega)(\partial \omega/\partial V)_0$ is the zero-temperature Gruneisen parameter [9]. The second temperature derivative $\tau \equiv (1/V)(\partial^2 V/\partial T^2)_0$ can also be expressed in terms of Γ and higher volume derivatives. Since it is somewhat more involved we present τ only for the case of a perfect Einstein crystal below:

$$\tau \equiv (1/V)(\partial^2 V/\partial T^2)_0 = 9(k_B)^2(1/B^2)(N/V)^2(2\gamma^3 - 2\gamma\gamma' - \delta\gamma^2) \tag{9}$$

where $\gamma' \equiv (V^2/\omega)(\partial \omega/\partial V)_0$ and $\delta = V[(\partial^3 U/\partial V^3)_0/(\partial^2 U/\partial V^2)_0]$.

It should be noted here that α, as well as higher temperature derivatives, can be expressed in terms of the correlation of energy and volume fluctuations that occur in finite-temperature, isobaric MC and MD simulations [7]. For example, one finds that

$$\alpha = V^{-1}(k_B \beta^2)\langle \delta V \, \delta H \rangle \tag{10}$$

where the volume fluctuation $\delta V = V - \langle V \rangle$ ($\langle V \rangle$ is the average volume) and the enthalpy fluctuation $\delta H = H - \langle H \rangle$. By expanding both V and H about the zero-temperature volume V_0 and taking the zero-temperature limit of the right-hand side of equation (10), one again obtains equation (8). Thus, the procedure outlined above is equivalent to that used in a histogram [6] or cumulant expansion [7] analysis, except that the reference temperature here is zero †.

Since the various parameters B, γ, δ and γ' can be calculated from a single energy minimization at zero temperature, it is possible, then, to determine $\langle V \rangle(T)$ over a wide temperature range from a $T = 0$ minimization. Further, quantities such as the equilibrium free energy, A, and the temperature dependence of the elastic properties of a solid can also be determined given $\langle V \rangle(T)$.

---

† These results can also be obtained from thermodynamics by noting that at all temperatures, from the chain rule, $(\partial V/\partial T)_p = (\gamma C_V/B)$ where $\gamma = V(\partial p/\partial E)_V$ and E is the internal energy. By differentiating again with respect to T at constant pressure p and using equation (1) for the free energy, one again arrives at equation (9) (for $T = 0$). This procedure requires several tedious applications of the chain rule. Therefore, it is possible to calculate α, τ and the higher temperature derivatives at non-zero temperatures from a single free-energy minimization.

2.2. Parabolic correction

As will be demonstrated below, quantities such as the equilibrium free energy and the bulk modulus can be determined quite accurately without having to determine $\langle V \rangle (T)$ to high accuracy. In order to do this we make use of the fact that A is a nearly parabolic function of V centred around the equilibrium volume $\langle V \rangle$. In fact, rather than calculating the higher-order temperature derivatives of the volume, it will be shown that $\langle V \rangle$ can be determined by using the predicted lower-order temperature derivatives, $(\partial V/\partial T)_0$ and $(\partial^2 V/\partial T^2)_0$, and the functional form of the LH free energy (equation (1)). A very accurate determination of $\langle V \rangle$ can be made by first using the temperature derivatives to determine a volume, V', that is close to (but not exactly at) the actual equilibrium volume, $\langle V \rangle$, and then simply evaluating the free energy at two additional values of V near V' and fitting the results to a parabola. That is, given V' and two other nearby volumes $V' \pm \epsilon$, then an excellent estimate of the equilibrium volume is

$$\langle V \rangle \approx V' - (\epsilon/2)[(f_1 - f_2)/(f_1 + f_2)] \tag{11}$$

where $f_1 \equiv A(V') - A(V' + \epsilon)$ and $f_2 \equiv A(V') - A(V' - \epsilon)$. The use of the parabolic fit here is justified because $|(V' - \langle V \rangle)/\langle V \rangle|$ is small.

In short, it is usually not necessary to calculate many of the higher-order temperature derivatives of the volume in equation (2) in order to determine most of the thermodynamic properties, including the defect properties. By using equations (8) and (9) along with equation (11) one can accurately determine the temperature dependence of the lattice parameter and then rescale the $T = 0$ relaxed atomic coordinates to obtain a good approximation to the finite-temperature structure and the properties of defects. This procedure neglects, of course, the excess local thermal expansion. For the defects considered below it will be shown that the effect of the excess local thermal expansion on most of the defect properties is small.

3. Simulation results

In order to validate the approach discussed above and determine its range of applicability, we determine some of the bulk thermodynamic and defect properties of solid Au. In this work we employ the EAM potential to model Au since such potentials have been used extensively to calculate both the bulk and the surface properties of pure metals and alloys successfully [10]. The EAM potential is given by

$$U = \sum_{i=1}^{N} F_i(\rho_i) + \frac{1}{2} \sum_{i=1}^{N} \sum_{j \neq i}^{N} \Phi(R_{ij}) \tag{12}$$

where R_{ij} is the distance between the particles i and j, $\Phi(R_{ij})$ is a pair potential and $F_i(\rho_i)$ is an embedding function that represents the energy needed to embed atom i in a uniform electron gas of density ρ_i.

In this work we consider three distinct types of defects: an isolated vacancy, a (100) free surface, and a $\Sigma 13$ [001] (22.62°) twist grain boundary. The vacancy was created by removing one atom from a three-dimensionally periodic simulation cell initially containing 256 atoms. The geometry of the cell used in the simulation of

the surface is described in detail elsewhere [11]. The two-dimensionally periodic simulation cell is divided into two regions, a region I in which the atoms respond to the interatomic forces and a region II in which the atoms are at their perfect-crystal positions. The surface was created by cleaving a perfect crystal to expose the (100) atomic plane. The geometry of the cell used to study the $\Sigma 13$ grain boundary is also described in detail elsewhere [11]. It consists of a region I containing the bicrystal and two region IIs in which the atoms are constrained to be at their perfect-crystal positions. The two crystals meeting at the grain boundary are free to translate with respect to one another by the addition of three extra variables in the minimization.

One procedure that was used to determine the thermodynamic properties over the temperature range of interest was to minimize the LH free energy (equation (1)) at each temperature with respect to the atomic coordinates and thereby determine the average positions of the atoms as a function of temperature. This procedure will be referred to as the LH free-energy minimization hereafter. For the case of a perfect crystal this procedure amounts to determining the dependence of the lattice parameter on temperature as the coordinates of the atoms are uniformly rescaled with temperature.

The results obtained with this procedure were then compared with those generated by performing only a single zero-temperature energy minimization in which the equilibrium crystal volume was determined by using the temperature derivatives of the volume (equations (8) and (9)). This procedure will be referred to as the zero-temperature energy minimization hereafter. For a perfect crystal the dimensionless γ and γ' were calculated by evaluating the frequency $\omega(V)$ at several volumes near the equilibrium $T = 0$ volume, V_0, and then differentiating numerically. The values of γ and γ' were found to be 2.650 and 2.252, respectively, for EAM Au. The dimensionless parameter δ was calculated by evaluating U at several volumes near V_0 and differentiating numerically. δ was found to be -6.2049. The $T = 0$ bulk modulus, B, (1.042 eV Å^{-3}) and volume, V_0, (67.917 Å^3) are inputs to the potential. For the defect calculations, the zero-temperature energy minimization procedure refers to the zero-temperature relaxed atomic positions of the defect system rescaled using $\langle a \rangle (T)$ for a perfect crystal as determined by using equations (8) and (9).
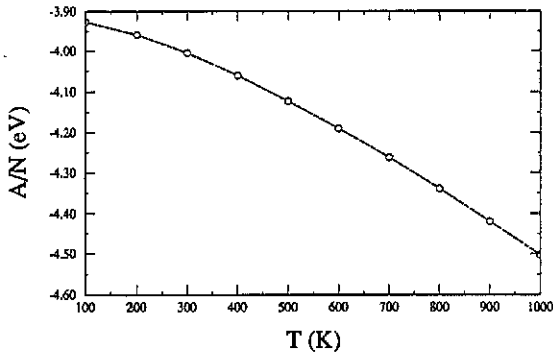
Finally, the results of the zero-temperature energy minimization were supplemented by performing a parabolic fit to the free energy and then using equation (11). This procedure will be referred to as the parabolic correction hereafter. As discussed in section 2.2 this procedure amounts to calculating the LH free energy at two volumes near the estimated equilibrium volume obtained from the zero-temperature energy minimization. Again, when referring to a defect, the parabolic correction procedure will mean that the zero-temperature atomic positions of the defect system are uniformly rescaled by using $\langle a \rangle (T)$ for a perfect crystal as determined by using the parabolic correction.

The first case we consider is a perfect FCC Au crystal under zero pressure. Figure 1 shows the dependence of the equilibrium lattice parameter, $\langle a \rangle (T)$, on the temperature T determined in three ways: by LH free-energy minimization at each temperature (circles), by zero-temperature energy minimization (broken curve), and by using the parabolic correction (full curve). As is evident from the figure, the $\langle a \rangle$ against T curve can be accurately determined over a temperature range of about 600 K from a single zero-temperature energy minimization. In addition, by using the explicit functional form of the local harmonic free energy and a simple parabolic fit one can obtain an extremely accurate fit over the entire temperature range from
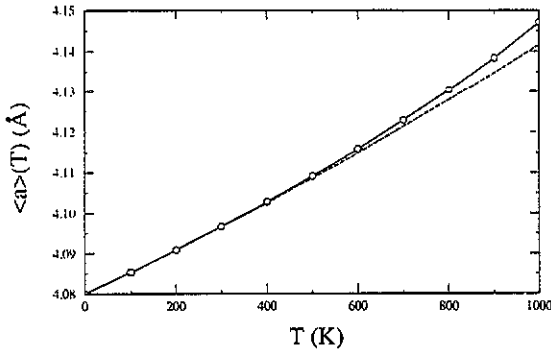
Figure 1. The equilibrium lattice parameter, $\langle a \rangle(T)$, of a perfect Au crystal plotted against temperature, T, determined by minimizing the local harmonic (LH) free energy (circles), by minimizing the zero-temperature energy and then calculating the temperature derivatives of the volume (broken curve), and by using the zero-temperature energy minimization results and the parabolic correction (full curve).

0 to 1000 K. Figure 2 is a plot of $A(T)$ against T as determined by a series of LH free-energy minimizations (circles) and by a single zero-temperature energy minimization (broken curve). Since $A(T)$ is essentially a parabolic function of a near its minimum, a discrepancy in the determination of $\langle a \rangle$ only affects $A(T)$ to second order in a. A similar calculation of A using the parabolic correction also leads to excellent agreement with the results of the LH free-energy minimizations.

Figure 2. The LH free energy, $A(T)$, of solid Au plotted against T as determined by a series of LH free-energy minimizations (circles) and by using the results of a zero-temperature energy minimization (broken curve). Note the good agreement between these approaches over a range of about 900 K.

The second case that we consider is that of an isolated vacancy in Au in a simulation cell containing 255 atoms. It is of interest to determine the dependence of the vacancy formation free energy, ΔA_v, on temperature since this quantity is needed to estimate, for example, the self-diffusion coefficient. The temperature dependence of the vacancy formation free energy ΔA_v is shown in figure 3 as determined by a series of LH free-energy minimizations (circles), by zero-temperature energy minimization (broken curve), and by using the parabolic correction (full curve). This figure shows that the results of rescaling the atomic positions using rather limited

zero-temperature information (the broken curve) can be used to predict ΔA_v accurately over a range of about 500 K. As for the temperature dependence of the perfect-crystal lattice parameter, incorporation of the parabolic correction results in extremely accurate vacancy formation energies over the entire temperature range examined ($0-10^3$ K). The good agreement between these various approaches reflects the fact that most of the relaxation of the atoms near the vacancy occurs when the system is relaxed at $T = 0$ K, and any additional temperature-dependent relaxation is both small and spatially localized. So, to a very good approximation, the temperature dependence of the vacancy formation energy can be determined by rescaling the relaxed zero-temperature structure of the defect system to that of the temperature of interest.
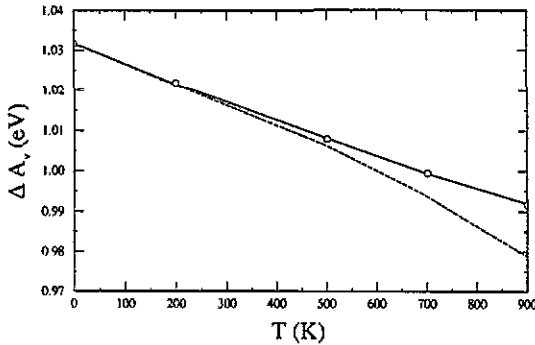

Figure 3. The vacancy formation energy, ΔA_v, plotted against T for an isolated vacancy in a 255-atom Au crystal calculated from a series of LH free-energy minimizations (circles), by zero-temperature energy minimization (broken curve), and by using a parabolic correction (full curve).

In order to see whether such a rescaling procedure could be used to obtain the temperature dependence of the properties of more extended defects we consider the case of a (100) free surface in Au. Figure 4 is a plot of the excess surface free energy (per unit area), $\gamma_s(T)$, as a function of temperature as determined by a series of LH free-energy minimizations (circles) and by using the parabolic correction (full curve). The results obtained by using these two approaches also agree remarkably well over the entire temperature range examined. This may seem surprising at first and, in fact, a detailed examination of the temperature dependence of the local thermal expansion for this system reveals that, as expected, there is a substantial excess local expansion near the surface. This is made more concrete in figure 5, where we show the temperature dependence of the spacing between the two (002) planes closest to the surface normalized by the temperature-dependent perfect-crystal lattice parameter $\langle a \rangle(T)$. This figure shows that there is, indeed, a small expansion near the surface that is not completely accounted for by the temperature dependence of the lattice parameter (less than 2%). Thus, even though there are spatially local deviations of the actual structure from the uniformly rescaled zero-temperature structure, these deviations do not substantially affect the surface free energy $\gamma_s(T)$.

The final and most complex case considered is a $\Sigma 13$ [001] (22.62°) twist grain boundary in the x–y plane. In figure 6 the temperature dependence of the excess grain boundary free energy per unit area, $\gamma_{gb}(T)$, is shown, as determined by a series of LH free-energy minimizations (circles) and by using the parabolic correction
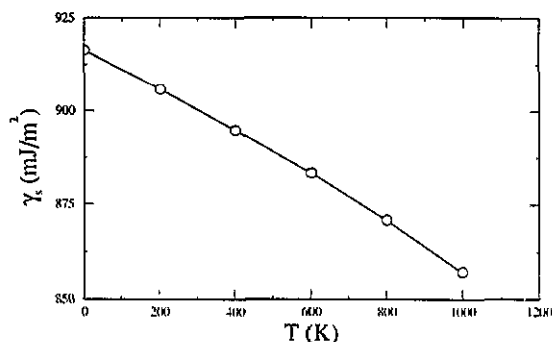
Figure 4. The excess surface free energy per unit area, $\gamma_s(T)$, of a (100) surface in Au plotted against T as determined by a series of LH free-energy minimizations (circles) and by rescaling the lattice parameter of the zero-temperature relaxed structure using $a(T)$ for the perfect crystal as determined by the parabolic correction (full curve). Note the good agreement between the results of these approaches despite the presence of local temperature-dependent relaxations.
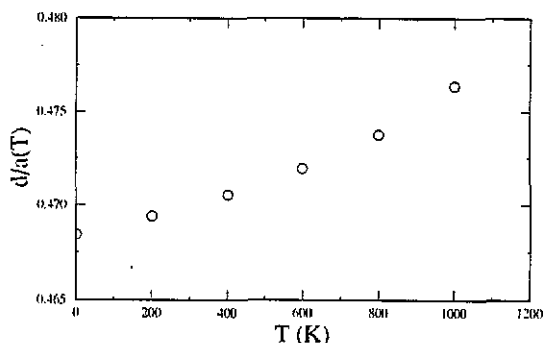
Figure 5. The ratio of the interplanar spacing to the perfect-crystal lattice parameter, $d/a(T)$, plotted against T for the two planes nearest the (100) free surface in Au. This shows that there are, indeed, local, temperature-dependent relaxations near the surface.

(full curve). Again, the results obtained by using these two approaches agree rather well over the entire temperature range. However, this agreement is not quite as good as for the perfect crystal, vacancy or surface. An analysis of the relaxed finite-temperature structure shows that this may be attributed to inhomogeneous, local temperature-dependent relaxations that cannot be wholly accounted for by the uniform bulk expansion $\langle a \rangle (T)$. In figure 7 we show the average positions of the atoms in planes adjacent to the grain boundary plane at 0, 600 and 1000 K. As is evident from the figure the additional temperature-dependent, in-plane relaxations of the atoms are rather small and so their effect on γ_{gb} is small. There is also a local temperature-dependent volume expansion at the grain boundary, the effect of which (on γ_{gb}) is probably somewhat more pronounced than the details of the local relaxation shown in figure 7.

4. Discussion and conclusions

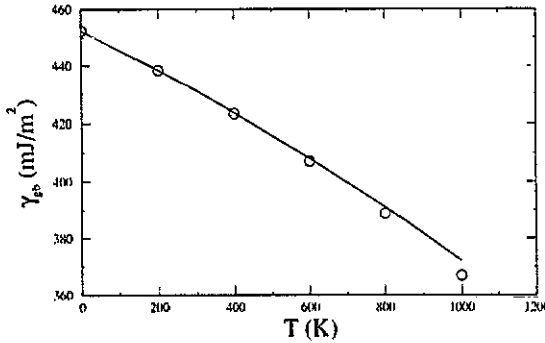We have shown that the temperature dependence of the structure and free energy

Figure 6. The excess grain boundary free energy per unit area, $\gamma_b(T)$, plotted against T for a $\Sigma 13$ [001] (22.6°) twist grain boundary in Au as determined by a series of LH free-energy minimizations (circles) and by rescaling the lattice parameter of the zero-temperature relaxed structure using $a(T)$ for a perfect crystal as determined by the parabolic correction (full curve). The results of these approaches agree over a range of about 800 K despite a temperature-dependent volume expansion at the grain boundary.
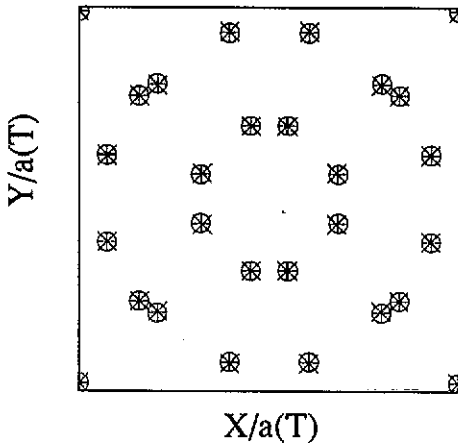

Figure 7. The in-plane positions of atoms in four planes that are adjacent to the $\Sigma 13$ [001] (22.6°) grain boundary plane at three different temperatures: O, 0 K; +, 600 K; X, 1000 K. Note that the in-plane temperature-dependent relaxations are small.

of both perfect crystals and defects can be accurately determined from a single zero-temperature energy minimization. For the case of a perfect crystal this was done by first expressing the temperature derivatives of the volume in terms of the volume derivatives of the vibrational frequencies of the solid, the interatomic potential and the zero-temperature structure. From this information it was possible to calculate $\langle V \rangle(T)$ or, equivalently, $\langle a \rangle(T)$ over a wide range in temperature. This temperature range was substantially extended by using the explicit functional form of the free energy and its shape near its minimum (the parabolic correction). It was also found that the free energy, $A(T)$, can be calculated to high accuracy from the zero-temperature structure since the free energy is nearly quadratic about the equilibrium volume such that small errors only affect $A(T)$ to second order in ΔV.

The bulk expansion $\langle a \rangle(T)$ for the perfect crystal was used to rescale the relaxed zero-temperature structure of defect systems uniformly to the temperature of interest and to thereby calculate the point-defect formation energy, the excess free energy of a (100) surface, and the excess free energy of a $\Sigma 13$ [001] (22.62°) twist grain boundary. Our results from single $T = 0$ simulations were found to be in excellent agreement

with those obtained by performing a series of LH free-energy minimizations for each defect over the same temperature range. This excellent agreement may be attributed to the fact that the temperature-dependent relaxations in these systems are often small, spatially localized and, as discussed above, because of the nearly parabolic shape of the free energy near its minimum.

It should be emphasized here that our procedure can also be applied to the quasi-harmonic free energy [12], which is a function of the full $(3N - 3) \times (3N - 3)$ dynamical matrix. In that case, the function $f(\omega)$ in equation (4) would be replaced by the (inverse of) the product of eigenfrequencies of the full dynamical matrix. In this way one can investigate the impact of making the local harmonic approximation on the thermodynamic properties of a system.

Although we have focused on determining thermodynamic information from the zero-temperature energy minimization, it is also possible (see earlier footnote) to obtain the thermal expansion, α, and higher temperature derivatives, such as τ, by performing a single LH free-energy minimization at some non-zero temperature, T. This approach would be necessary if, for example, one were interested in determining the properties of a solid phase that was stable only at high temperatures. In the appendix we demonstrate that the temperature dependence of the lattice parameter, $\langle a \rangle$, of Au can be calculated from a single free-energy minimization, in this case at $T = 500$ K.

Although the method described here enables one to calculate a great deal of finite-temperature thermodynamic information from a zero-temperature energy minimization it does have its limitations at high temperatures and in some defect systems where local, temperature-dependent relaxations are large. At high temperatures ($T \gg \Theta_D$, where Θ_D is the Debye temperature) the local harmonic description should strictly be modified to include contributions from the higher-order anharmonic terms in the energy. Nevertheless, the LH description captures much of the anharmonicity and permits an accurate calculation of both perfect crystal and defect properties, even at high temperatures [4]. Future research will focus on determining the temperature dependence of local relaxations from the zero-temperature relaxed structure.

Acknowledgments

Appendix

In this appendix the temperature dependence of $\langle a \rangle$ for Au is determined by calculating its thermal expansion, α, at $T = 500$ K and then using a parabolic correction. In order to apply equation (8) at this temperature it is necessary to calculate both the Gruneisen parameter, γ, and the bulk modulus, B. The former is calculated, as before, by evaluating the frequency, ω, at several volumes near the equilibrium volume and then differentiating numerically. The latter is calculated by evaluating the LH free energy, A, at several volumes near the equilibrium volume and determining its second volume derivative from a fit to the data. We find that $\gamma = 2.823$
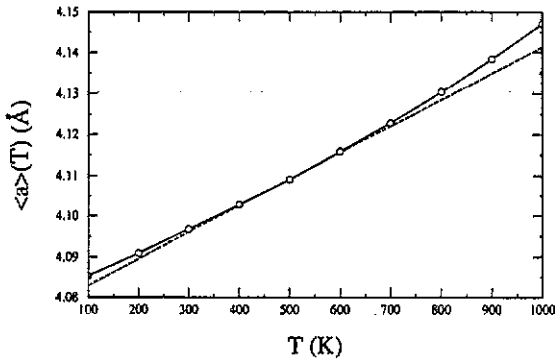
Figure A.1. The lattice parameter, $\langle a \rangle (T)$, as a function of temperature as determined by a series of LH free-energy minimizations, by a single free-energy minimization at $T = 500$ K in which α is calculated, and by using a parabolic correction.

and $B = 0.887$ eV Å^{-3}. The temperature dependence of the lattice parameter, as determined by a series of LH free-energy minimizations (circles), by a single LH free-energy minimization at $T = 500$ K in which only α is calculated (dotted line), and by a parabolic correction (full curve), is shown in figure A.1. The excellent agreement between the finite-temperature simulation results and those obtained from the parabolic correction to the 500 K thermal expansion indicates that the present approach is equally applicable based upon either a single $T = 0$ or finite-temperature simulation.

References

[1] Frenkel D and Ladd A J C 1984 *J. Chem. Phys.* **81** 3188
[2] Squire D R, Holt A C and Hoover W G 1969 *Physica* **42** 388
[3] Squire D R and Hoover W G 1969 *J. Chem. Phys.* **50** 701
[4] LeSar R, Najafabadi R and Srolovitz D J 1989 *Phys. Rev. Lett.* **63** 624
[5] Sutton A P 1989 *Phil. Mag.* A **60** 147
[6] Ferrenberg A M and Swendsen R H 1988 *Phys. Rev. Lett.* **61** 2635
[7] Rickman J M and Phillpot S R 1991 *Phys. Rev. Lett.* **66** 349
[8] Pathria R K 1984 *Statistical Mechanics* (New York: Pergamon)
[9] Kittel C 1976 *Introduction to Solid State Physics* (New York: Wiley)
[10] Foiles S M, Daw M S and Baskes M I 1986 *Phys. Rev.* B **33** 7983
[11] Najafabadi R, Wang H Y, Srolovitz D J and LeSar R 1991 *Acta Metall.* **39** 3071
[12] Barron T H K and Klein M L 1974 *Dynamical Properties of Solids* vol 1, ed G K Horton and A A Maradudin (Amsterdam: North-Holland) pp 391–450